scientific reports

Check for updates

OPEN

Evaluation of blood-tumor barrier permeability and doxorubicin delivery in rat brain tumor models using additional focused ultrasound stimulation

Hyo Jin Choi[1,5], Mun Han[1,5], Byeongjin Jung[1,2], Hyungkyu Huh[1], Eun-hee Lee[1], Jong-ryul Choi[1] & Juyoung Park[3,4]✉

Focused ultrasound (FUS) has emerged as a promising technique for temporarily disrupting the blood-brain barrier (BBB) and blood-tumor barrier (BTB) to enhance the delivery of therapeutic agents. Despite its potential, optimizing FUS to maximize drug delivery while minimizing adverse effects remains a significant challenge. In this study, we evaluated a novel FUS protocol that incorporates additional FUS stimulation without microbubbles (MBs) ("FUS protocol") prior to conventional BBB disruption with MBs ("BBBD protocol") in a rat brain tumor model (n = 35). This approach aimed to validate its effectiveness in enhancing BBB/BTB disruption and facilitating doxorubicin delivery. T1-weighted contrast-enhanced and dynamic contrast-enhanced (DCE) MRI demonstrated significant increases in signal intensity and permeability (K_{trans}) in the tumor region under the "FUS + BBBD protocol", with 2.65-fold and 2.08-fold increases, respectively, compared to the non-sonicated contralateral region. These values were also elevated compared to the conventional "BBBD protocol" by 1.45-fold and 1.25-fold, respectively. Furthermore, doxorubicin delivery in the targeted region increased by 1.91-fold under the "FUS + BBBD protocol", compared to a 1.44-fold increase using the conventional "BBBD protocol". This novel FUS approach offers a promising, cost-effective strategy for enhancing drug delivery to brain tumors. While further studies are required to assess its applicability with different chemotherapeutics and tumor types, it holds significant potential for improving brain tumor treatment in both preclinical and clinical settings.

Keywords Focused ultrasound, Blood-tumor barrier, Mechanical stress, Doxorubicin, Dynamic contrast-enhanced magnetic resonance imaging (DCE-MRI)

The blood-brain barrier (BBB) is an obstacle to the effective treatment of brain tumors because it limits drug delivery and penetration[1,2]. Vigorous angiogenesis in tumors forms a heterogeneous vasculature with a compromised BBB, the so-called blood-tumor barrier (BTB)[3]. Due to its permeability, the BTB allows for the extravasation of small and large molecules[4–7]. However, the BTB permeability is highly heterogeneous depending on the type, stage, and lesion of the brain tumor. Hence, the controlled delivery of adequate amounts of therapeutic agents for tumor treatment remains unclear[7,8].

Radiation therapy combined with chemotherapy is currently used as the international standard of care for brain tumor treatment. Alternative methods, such as mannitol and bradykinin, have been attempted to increase the amount of therapeutic agent delivery for effective tumor treatment[9]. However, limitations such as unpredictable BBB disruption can pose a potential risk to normal brain tissue[10]. Various experimental approaches, including

[1]Medical Device Development Center, Daegu-Gyeongbuk Medical Innovation Foundation (K-MEDI hub), 80 Cheombok-ro, Dong-gu, Daegu 41061, Republic of Korea. [2]BioHealth Convergence Center, Daegu Technopark, 46-17 Seongseogongdan-ro, Dalseo-gu, Daegu 42716, Republic of Korea. [3]College of IT Convergence, Department of Biomedical Device, Gachon University, 1342, Seongnam-daero, Sujeong-gu, 1342, Seongnam 13120, Gyeonggi, Republic of Korea. [4]Neumous Inc., 1526, Seongnam-daero, Sujeong-gu, Seongnam-si 13113, Gyeonggi-do, Republic of Korea. [5]These authors contributed equally: Hyo Jin Choi and Mun Han. ✉email: opedoors@gachon.ac.kr

the use of viral vectors[11], polymeric nanoparticles[12], and exosomes[13], have also been investigated to improve drug delivery across the BBB and BTB (hereafter referred to as BBB/BTB)[14]. Unfortunately, these methods are not yet used in clinical practice owing to some limitations such as difficulties in manufacturing, high production cost, safety[15,16] and therapeutic efficacy due to low accumulation[17].

Focused ultrasound (FUS) combined with intravenously injected microbubbles (MBs) has recently emerged as a promising non-invasive approach for disrupting the BBB/BTB. Preclinical studies using glioma models in animals have demonstrated its potential to enhance the delivery of therapeutic agents, including trastuzumab[18], doxorubicin[19], temozolomide[20], methotrexate[21], and carboplatin[22], to targeted brain tumor regions. These studies have shown tumor suppression and improved survival rates in rat and mouse brain tumor models. Additionally, several clinical studies have confirmed the safety and feasibility of focused ultrasound BBB disruption (FUS-BBBD) using various devices, multiple treatment sessions, and various chemotherapies in patients with newly diagnosed GBM, recurrent GBM, and high-grade gliomas[23]. Despite the progress made in preclinical and clinical trials, further optimization of FUS parameters, including exposure settings and MB doses, is needed to minimize the risk of hemorrhage and other adverse effects while maximizing therapeutic outcomes[24–26].

We previously reported that an additional FUS stimulation ("FUS protocol") step without MB injection prior to the conventional BBBD ("BBBD protocol") enhances BBB permeability and doxorubicin (DOX) delivery to the brain of healthy rats without damaging nearby tissues or vessels[27]. However, the robustness of this new FUS protocol ("FUS + BBBD protocol") has not been validated in the tumor microenvironment. As a follow-up study, we tested the efficacy and efficiency of the FUS+BBBD protocol in the tumor rat model.

Methods

Animals and husbandry

All experiments were approved by the Animal Experiment Ethics Committee of Daegu–Gyeongbuk Medical Innovation Foundation (IACUC No. DGMIF-20122901-00). All procedures were conducted in accordance with the relevant guidelines. The study was also conducted in compliance with the ARRIVE (Animal Research: reporting of in vivo experiments) guidelines (https://arriveguidelines.org/arrive-guidelines). All efforts were made to minimize the number of animals used and their pain.

Male Sprague-Dawley rats (5 weeks old, weighing 100–150 g for tumor drug delivery study, $n = 63$) were purchased from Orient Bio Inc. (Sungnam, Republic of Korea). All rats were used after 7 days of acclimatization in the vivarium of the Laboratory Animal Center (LAC) of the Daegu-Gyeongbuk Medical Innovation Foundation (DGMIF). Rats were fed a normal diet with water during acclimatization. The temperature (20–25 °C) and humidity (40–45%) were controlled, and a 12:12 h light/dark cycle was maintained in polycarbonate cages. The rats used in this study were randomly divided into five groups based on the sonication protocol (Table 1).

Reagents

Doxorubicin hydrochloride (DOX) (Boryung Pharmaceutical, Seoul, Republic of Korea) was used to confirm drug delivery in the tumor environment. Evans blue (Sigma-Aldrich St. Louis, MO, USA) was used to demonstrate the BBB opening region. Zoletil (Virbac Laboratories, Carros, France) and Rompun (Bayer, Leverkusen, Germany) were used for animal anesthesia. Microbubbles (MBs) Definity® were purchased (Lantheus Medical Imaging, North Billerica, MA, USA) for BBB opening along with FUS, and gadoterate meglumine (Gd-DOTA) was purchased (Dotarem®; Guerbet, Roissy CDG, France) to identify the BBB opening region using MRI.

9L gliosarcoma cell culture

9L gliosarcoma cell lines (ATCC® CRL-2200™) were cultured at 37 °C and 5% CO_2 in Dulbecco Modified Eagle Medium (DMEM; 11995-073, Gibco, Gaithersburg, MD, USA) supplemented with 10% fetal bovine serum

Experimental purpose	Sonication protocol	Animal number
BBB permeablization (T1 and DCE-MRI)	Ctrl	4
	1.0 F	4
	B	4
	1.0FB	4
Drug delivery	Ctrl	12
	1.0 F	5
	B	8
	0.5FB	5
	1.0FB	8
	2.0FB	6
Histopathology	1.0 F	3
	B	
	1.0FB	

Table 1. Summary of the sonication protocol groups. 1.0 F: 1.0 MPa w/o MB; B: 0.72 MPa w/ MB; 0.5FB: 0.5 MPa w/o MB + 0.72 MPa w/ MB; 1.0FB: 1.0 MPa w/o MB + 0.72 MPa w/ MB; 2.0FB: 2.0 MPa w/o MB + 0.72 MPa w/ MB.

(FBS; 16000-044, Gibco, Gaithersburg, MD, USA) and 1% penicillin-streptomycin (PS; 15140-122, Gibco, Gaithersburg, MD, USA), as previously described[20,28,29]. At approximately 90% cell confluence, the medium was removed and the cells were detached using 0.25% trypsin-EDTA (25200-056, Gibco, Gaithersburg, MD, USA). To prepare the tumor cells for implantation, they were centrifuged at 1,000 rpm for 2 min, suspended in DMEM at a final concentration of 5×10^5 cells/5 µL, and kept cool until implantation. Before tumor implantation, the 9L gliosarcoma stock was thawed and used for the experiment after the acclimatization period. All brain tumor implantations were carried out with 9L gliosarcoma at passage number 5–7.

Brain tumor implantation procedure

The rats were anesthetized with an intramuscular injected anesthetic mixture [Zoletil (25 mg/kg): Rompun (4.6 mg/kg): saline = 5:2:3] prior to tumor implantation. The rat was fixed to the stereotaxic frame (Harvard Apparatus, Holliston, MA, USA) using an in-ear and upper tooth bar for hemostasis. Animal hair was shaved, and a sagittal incision was made on the posterior aspect of the head, approximately 2 cm. A small burr hole was drilled using a dental drill (Saeshin, Daegu, Korea) 3 mm lateral and 1 mm anterior to the *bregma*. The 9L gliosarcoma cells filled in a 25 µl Hamilton syringe (Hamilton Company, Reno, NV, USA) were slowly injected at 5 mm under the dura mater at a flow rate of 1 µL/min for 5 min using a 30 gauge Hamilton needle (Hamilton Company, Reno, NV, USA) and a syringe pump (Harvard Apparatus, Holliston, MA, USA). To avoid any cell leakage or backflow of the media, holes were filled with Hy-bond polycarboxylate cement (Shofu, TYOKO, Japan) and the skin was sutured. After 10–14 days of implantation, tumor size was checked using a horizontal bore 9.4T animal MRI (BioSpec 94/20 USR; Bruker, Billerica, MA, USA) for controlled experiments. A total of 35 rats that presented with a tumor diameter of 1.5 ~ 2.0 mm based on T2-weighted (T2W) coronal images were selected and used in the experiment.

MRI-guided focused ultrasound (MRgFUS) system

The MRgFUS system (RK-100; FUS Instruments, Toronto, Canada) was used to sonicate rat brains for the BBB as described previously[27,30]. A schematic of the system is presented in Fig. 1. Briefly, the system has an air-back, single-element, and spherical piezoelectric transducer (FUS Instruments, Toronto, Canada). A spherical piezoelectric transducer with a diameter of 75 mm and a radius of curvature of 60 mm, which generates a resonant frequency of 1 MHz, was used. The ultrasound − 3 dB acoustic pressure width and length of the focal region were 1.5 mm and 6 mm in free water at the peak pressure measured by the Acoustic Intensity Measurement System (AIMS III, ONDA, Sunnyvale, CA, USA) and the hydrophone (HGL-400, ONDA, Sunnyvale, CA, USA)[30]. The transducer was driven by a waveform generator (33220 A; Agilent, Santa Clara, CA, USA) and an RF power amplifier (4010 L; E&I, Rochester, NY, USA). The transducer was submerged in a degassed water tank. A 9.4T MRI and a volume coil with an 86-mm inner diameter were used for image guidance by synchronizing the coordinates between the two systems (MRI and MRgFUS system).

Sonication protocol

Sonication was performed using the MRI-guided focused ultrasound (MRgFUS) system, as described in the Methods section. Burst sonication (10ms tone burst, pulse repetition frequency (PRF) of 1 Hz for 120 s) was performed at the location of the tumor. The acoustic pressure of the FUS protocol "F" was 0.5, 1.0, and 2.0 MPa depending on the experimental purpose (Table 1) and the acoustic pressure of the BBBD protocol "B" was 0.72 MPa. The FUS + BBBD protocol "FB" was a fusion of both, where "FUS protocol" ultrasound was applied prior to the "BBBD protocol" without MB injection. The details of the experimental schedule for the sonication protocols are presented in Fig. 2. These sonication parameters have been verified as safe conditions in previous studies[27,30,31]. Although BBB/BTB is simultaneously disrupted in the tumor animal model, the protocol used in this study is referred to as BBBD throughout the manuscript in order to minimize confusion and to be consistent with previous studies.

Magnetic resonance imaging

A 9.4T preclinical animal MRI was used for magnetic resonance imaging. T1-weighted (T1W) MR images were used to check the BBB disruption. T2-weighted (T2W) MR images were used as a guide for ultrasound targeting and tumor size checking. Meanwhile, DCE-MRI was used to identify the permeability[19,27,30]. MRI parameters were as follows: T1W, echo time (TE) = 6.5 ms, repetition time (TR) = 1500 ms, field of view (FOV) of 40×40 mm^2, matrix size of 256×256, axial and coronal slices of 1.5 mm slice thickness without a gap, and the number of excitations (NEX) = 3. T2W: TE = 33 ms, TR = 2500 ms, FOV = 40×40 mm^2, matrix size = 256×256, axial and coronal slices of 1.5 mm slice thickness without a gap, and NEX = 2. DCE-MRI: TE = 1.5 ms, TR = 24.3 ms, FOV = 40×40 mm^2, matrix size of 128×128, axial and coronal slices with 1.5 mm slice thickness without a gap, and NEX = 3. The MRI parameters are summarized in Table 2.

The region of interest (ROI), which is the focal area of the transducer, was selected as a circle with a diameter of 1.5 mm. The relative signal intensity R_t of the tumor region at a given time point ($T1_t$) was normalized by the signal intensity of pre-injection T1W MR images (0 min, $T1_{pre}$) using the following equation:

$$R_t\,(\%) = \frac{(T1_t - T1_{pre})}{T1_{pre}} * 100$$

The BBB permeability K_{trans} was calculated based on a Patlak model using DCE-MRI images, similar to a previous study[32]. T1 measurements were acquired using (RARE VTR) (TR = 160, 180, 200, 250, 300, 400, 500, 600, 700, 800, 900, 1000, 1200, 1500, 1800, 2000, 2500, 3000, 3500, 4000, 6000, and 12000 ms). Ten sets of FLASH images were acquired before the contrast agent injection (Gd-DOTA with relaxivity of 3.0 $s^{-1}mM^{-1}$), followed by 90

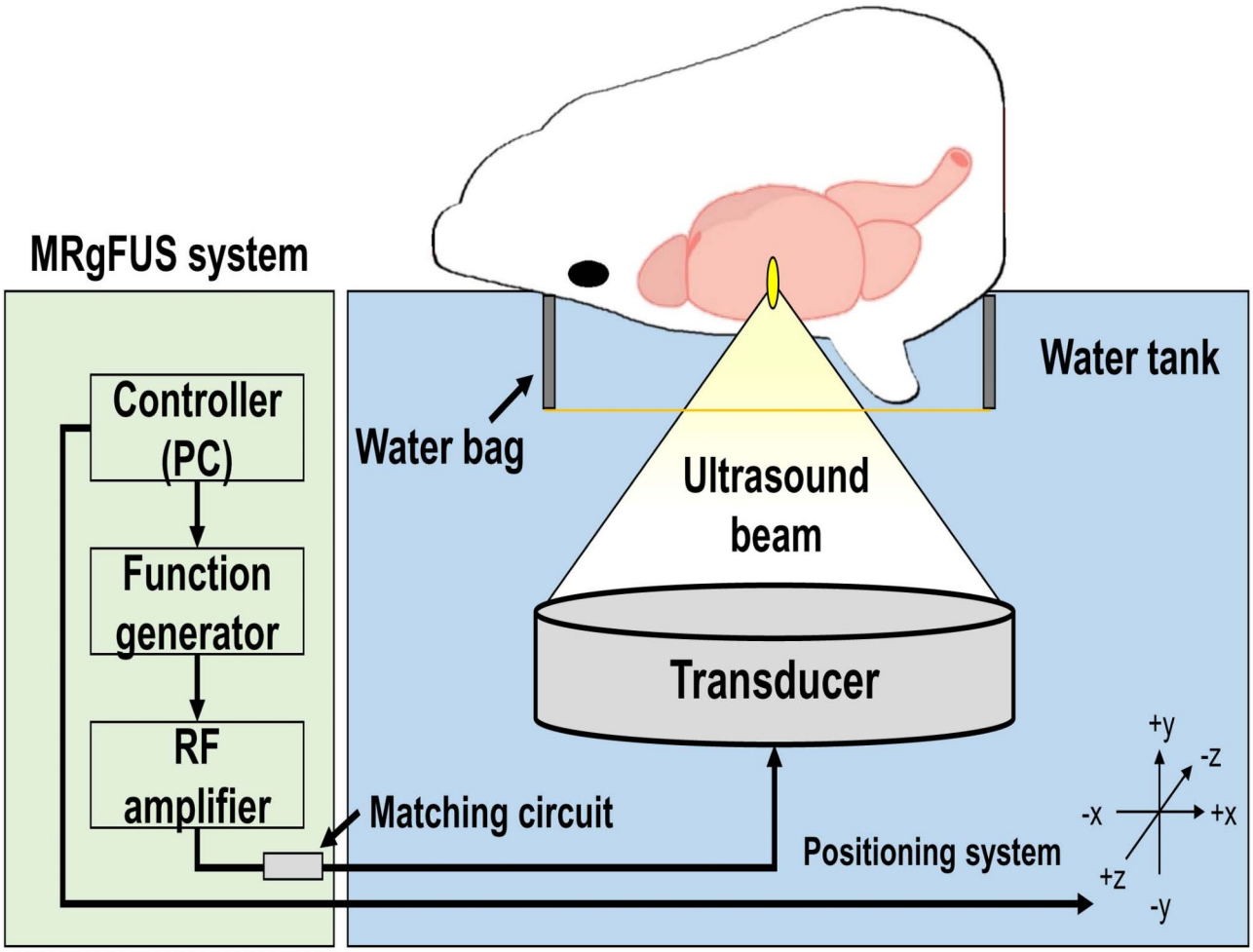

Fig. 1. Schematic of the MRgFUS system for BBBD. The sonication region was targeted using MRI and the transducer position was controlled in synchronization with the MRgFUS system.

sets of FLASH images acquired during and after CA injection with a temporal resolution of 9.32 s for 10 min. T1 mapping and DCE-MRI were performed at the same slice position. Identical regions of interest (ROIs) were designated on two slices, resulting in the extraction of two data points per subject. The ROI was selected using a 5-pixel circle diameter, which corresponds to a 1.5 mm focal area of the transducer (3.2 pixels/mm). The plasma concentration of the contrast agent was measured in a large blood vessel (ophthalmic artery or transverse sinus). The hematocrit level was assumed to be 45% in the capillary[33].

Blood-brain barrier disruption experiment

The blood-brain barrier and blood-tumor barrier disruption experiments were performed as described in our previous studies[27,30]. Before sonication, the tumor size was checked with T1-weighted MR images 10–14 days after tumor implantation. A tumor diameter of 1.5 ~ 2.0 mm was selected and used in this study. Briefly, rats were anesthetized with an intramuscular injection of an anesthetic mixture (Zoletil (25 mg/kg): Rompun (4.6 mg/kg): saline = 5:2:3). After anesthesia, an angiocatheter was inserted into the vein of the tail, and the hair on the head was shaved. Then, the rat was placed in a supine position on an MR-compatible plastic bed, and the exposed scalp was immersed in a degassed water bag using fixed ear and tooth bars (Fig. 1). Sonication of the tumor region was performed according to the protocol described in Fig. 2. The T2W MR image was scanned and registered with the MRgFUS system and placed in sync. The 0.02 mL/kg perflutren lipid MB (Definity®) was diluted 1:50 in saline and administered through an angiocatheter using an automated syringe pump (Harvard Apparatus, Holliston, MA, USA). Sonication was then started 10 s after the diluted MB solution infusion. Following sonication, T1W MR or DCE-MR images were performed to identify BBBD and permeability with Gd-DOTA (0.2 mM/kg). DOX (5.67 mg/kg) and Evans blue (4 mg/kg) were administered intravenously (i.v.) to mark the DOX delivered region for tissue extraction.

Doxorubicin quantification

All rats were sacrificed 24 h after the IV administration of DOX and perfused with 0.9% NaCl via transcardial perfusion followed by brain extraction. Then, the sample volume (approximately 30 mg of tissue) of the

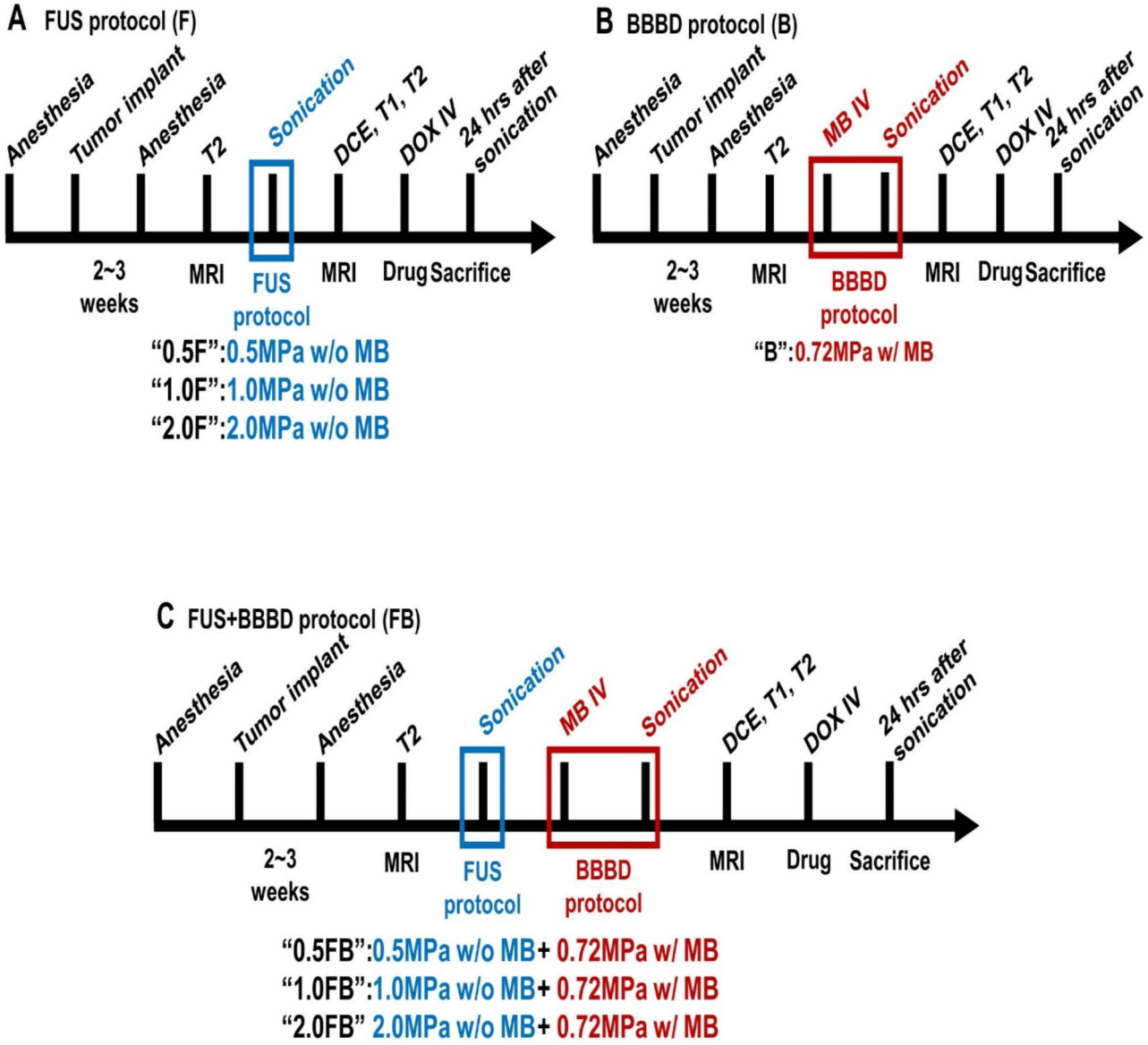

Fig. 2. Experimental timeline of (**A**) FUS protocol, (**B**) BBBD protocol, and (**C**) FUS + BBBD protocol. Each bar indicates experimental steps from animal anesthesia to sacrifice. The blue and red boxs and text indicate FUS and BBBD sonication, respectively (*MB* microbubbles, *DOX* doxorubicin, *EB* Evans blue).

Sequence	Use	TE* (ms)	TR** (ms)	FOV*** (mm2)	Matrix size	Slice thickness (mm)	NEX****
RARE T1-weighted	Detection of BBB disruption	6.5	1500	40 × 40	256 × 256	1.5	3
RARE T2-weighted	Sonication target planning/detection of edema/tumor size checking	33	2500	40 × 40	256 × 256	1.5	2
FLASH DCE-MRI	Permeability measurement	1.5	24.3	40 × 40	128 × 128	1.5	3

Table 2. MR imaging parameters. *TE: Echo time; **TR: Repetition time; ***FOV: Field of view; ****NEX: Number of excitations.

tumor region was harvested for quantification. The tumor samples were homogenized with acidified ethanol (50% ethanol in 0.3 N HCl) using a bead beater and incubated for 24 h at 4 °C. After incubation, the samples were centrifuged at 16,000×*g* for 20 min to remove the tissue pellet, and the supernatant was collected. The fluorescence intensity was measured using a fluorometric detector with 480 nm excitation and 590 nm emission (Infinite 200 Pro; TECAN, Austria GmbH, Austria). The concentration of DOX was quantified using a standard curve derived from eight serial concentrations of pure DOX (0, 10, 20, 50, 100, 200, 500, and 1000 ng/mL).

Fluorescence intensity was analyzed using TECAN i-Control Software (TECAN, Austria GmbH, Austria), and all measurements were repeated at least three times. The contralateral tumor region without sonication was used as a control to correct autofluorescence. DOX fluorescence detection and analysis were performed as described previously[27,31,34].

Hematoxylin and Eosin (H&E) staining

Histopathological changes in the sonicated rat brain tissue were investigated by H&E staining as described previously[19,30,32]. The sonicated rats were sacrificed 24 h post-sonication, followed by transcardiac perfusion with 0.9% NaCl and fixation with 10% formalin. The rat brains were extracted and fixed in 10% formalin for 7 days. The brain tissue samples were then embedded in paraffin and cut serially in 4 μm thickness axial direction using a microtome (HistoCore AUTOCUT; Leica, Wetzlar, Germany). Paraffin-embedded sections were deparaffinized and rehydrated before staining. Brain tissue slides were stained with an H&E stain kit (Vector Laboratories, Burlingame, CA, USA). Images were taken with a digital slide scanner (Axio Scan.Z1; Carl Zeiss, Oberkochen, Germany).

Statistical analysis

The values obtained were expressed as mean ± standard deviation. Statistical differences between the control group and experimental groups were compared using a two-tailed paired t-test, one-way ANOVA with Tukey's test, and two-way ANOVA with Tukey's test and Mann-Whitney U test using GraphPad Prism 8 (GraphPad Software, Inc., San Diego, CA, USA). Statistical significance was accepted for p-values < 0.05.

Results

BBB/BTB permeability

To investigate the effect of the additional FUS stimulation on the BBB/BTB permeability, contrast-enhanced T1W MR imaging was performed for "B", "1.0FB", and "1.0F" as shown in Fig. 3. Representative MR Images of each case show the average signal intensity of the contrast agent after BBB/BTB disruption (Fig. 3A). For every given case, the averaged signal intensity of the sonicated tumor region was higher than the non-sonicated contralateral "C" region in both "B" and "1.0FB" cases. However, this difference was not observed for the "1.0F" case. To quantify the BBB/BTB permeability, the relative signal intensity of the contrast agent was measured in a time-dependent manner (before, 0, 3, 5, 7, 9, and 11 min), as shown in Fig. 3B. The relative signal intensity of the target area increased by 33.2 ± 3.1%, 41.2 ± 3.1%, 43.9 ± 3.3%, 45.9 ± 3.0%, 44.9 ± 2.7% and 55.0 ± 4.9%, 54.5 ± 3.4%, 51.1 ± 1.3%, 48.9 ± 0.7%, 47.9 ± 0.1% for each time point compared to the contralateral region under "B" and "1.0FB" protocol, respectively. However, the "1.0F" region showed no significant change compared to the contralateral "C" region. In these results, the relative signal intensity was highest (2.65 times higher than the contralateral region) at the "1.0FB" region, 3 min after the MR contrast agent injection.

In addition to the averaged signal intensity changes, brain permeability (K_{trans}) was calculated using DCE-MRI for each protocol ("B", "1.0FB", and "1.0F"). The representative K_{trans} map and group-averaged K_{trans} values before and after the sonication procedure are shown in Fig. 4A and B. The baseline pre-sonication K_{trans} values in the tumor region were measured to be 0.04263 ± 0.00756 min^{-1} for the "B" protocol and 0.04453 ± 0.00694 min^{-1} for the "FB" protocol. The average permeability of the tumor region (n = 4) after sonication was enhanced by 0.0741 ± 0.0159 min^{-1} and 0.0928 ± 0.0186 min^{-1} for the "B" and "FB" protocols, respectively. This corresponds to a 1.73-fold increase for the "B" protocol and a 2.08-fold increase for the "FB" protocol relative to the baseline pre-sonication values (Fig. 4C). The increase in K_{trans} after sonication was statistically significant (p = 0.031 and 0.0006 for "B" and "1.0FB" protocols, respectively). For the "1.0F" protocol, however, no significant increase in the brain permeability was observed (0.0379 ± 0.00701 $min^{[-1}$ after sonication, compared to 0.0378 ± 0.00738 $min^{[-1}$ before sonication with p = 0.99).

DOX delivery

The targeted brain tissue samples were measured for statistical comparison for DOX delivery for each protocol "B", "1.0FB", and "1.0F" as shown in Fig. 5. The average DOX concentration was 694.1 ± 398.5 ng/g in the contralateral "C" region, while it was 885.1 ± 305.6 ng/g in the tumor region sonicated with "B", 996.2 ± 408.0 ng/g for "0.5FB", 1255.4 ± 347.8 ng/g for "1.0FB", 1327.8 ± 470.7 ng/g for "2.0FB", and 757.3 ± 447.4 ng/g for "1.0F". The amount of DOX delivered under the "B", "0.5FB", "1.0FB", "2.0FB", and "1.0F" protocols was 1.28 ± 0.44, 1.44 ± 0.59, 1.81 ± 0.50, 1.91 ± 0.68, and 1.09 ± 0.64 times higher, respectively, than in the contralateral region without sonication "C".

Histopathological analysis

H&E histopathological analysis (n = 3) was performed to identify the damage caused by "B", "1.0FB", and "1.0F" in the brain tumor region. No significant differences between regions sonicated with each protocol were observed in the 5-and 20 times magnified images, as shown in Fig. 6.

Discussion

There are increasing clinical demands[35–37] on safe and efficient drug delivery techniques for tumor treatment. A temporal BBB/BTB opening using focused ultrasound was suggested as a possible candidate[38–40]. Previous research demonstrated that incorporating an additional sonication step prior to conventional BBBD can enhance drug delivery in healthy rat brains by up to 1.75 times, without inducing tissue damage or heating[27]. This additional sonication step, performed without microbubble injection, has been shown to be a simple yet

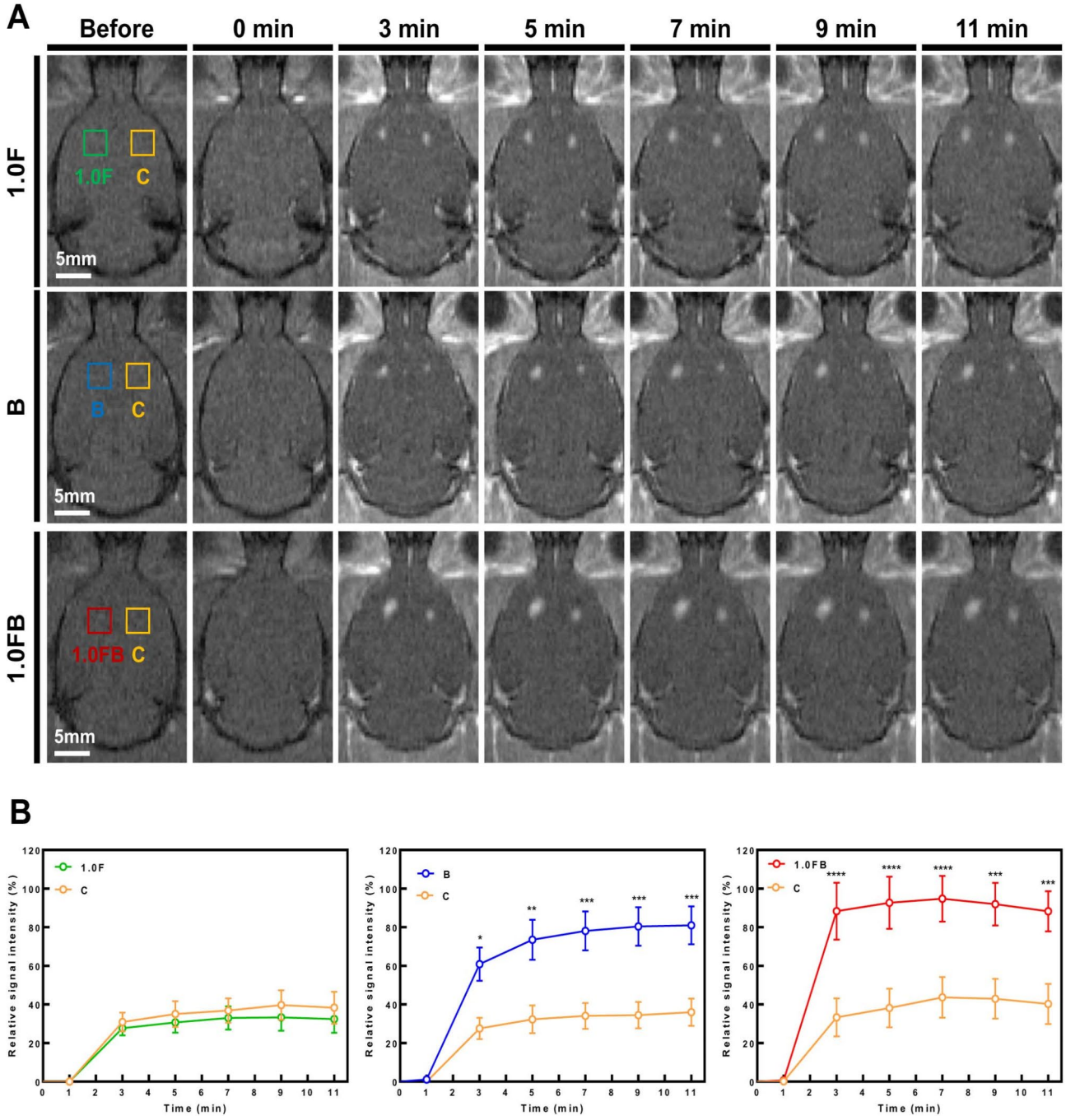

Fig. 3. (**A**) Representative T1-weighted MR images for each protocol ("1.0F", "B", and "1.0FB") taken before and at 0, 3, 5, 7, 9, and 11 min after contrast agent injection. (**B**) A relative signal intensity changes at the sonicated region. Scale bars represent 5 mm. (Signal intensity: "C" $n = 4$, Yellow box, line, and circle; "1.0F" $n = 4$, Green box, line, and circle; "B" $n = 4$, Blue box, line, and circle; "1.0FB" $n = 4$, Red box, line, and circle). $^{*}p < 0.05$, $^{**}p < 0.01$, $^{***}p < 0.001$, $^{****}p < 0.0001$ vs. "C." Values of $p < 0.05$ were considered as statistically significant.

effective means of increasing drug delivery. The present study focuses on validating this protocol in tumor models, aiming to support its potential translation into clinical applications.

Consistent with previous experiments in normal rats, the addition of ultrasound sonication significantly enhanced BBB/BTB opening in the tumor environment. Given that the BTB is known to be more permeable than the intact blood-brain barrier[4–7], baseline BTB permeability was assessed through MR imaging 24 h prior to sonication to minimize experimental bias. Using the "1.0FB" protocol, the signal intensity of T1-weighted MR and K_{trans} increased by approximately 2.42-fold and 2.08-fold, respectively, compared to pre-sonication measurements at the same target, and by 2.65-fold and 2.15-fold relative to the contralateral tumor region.

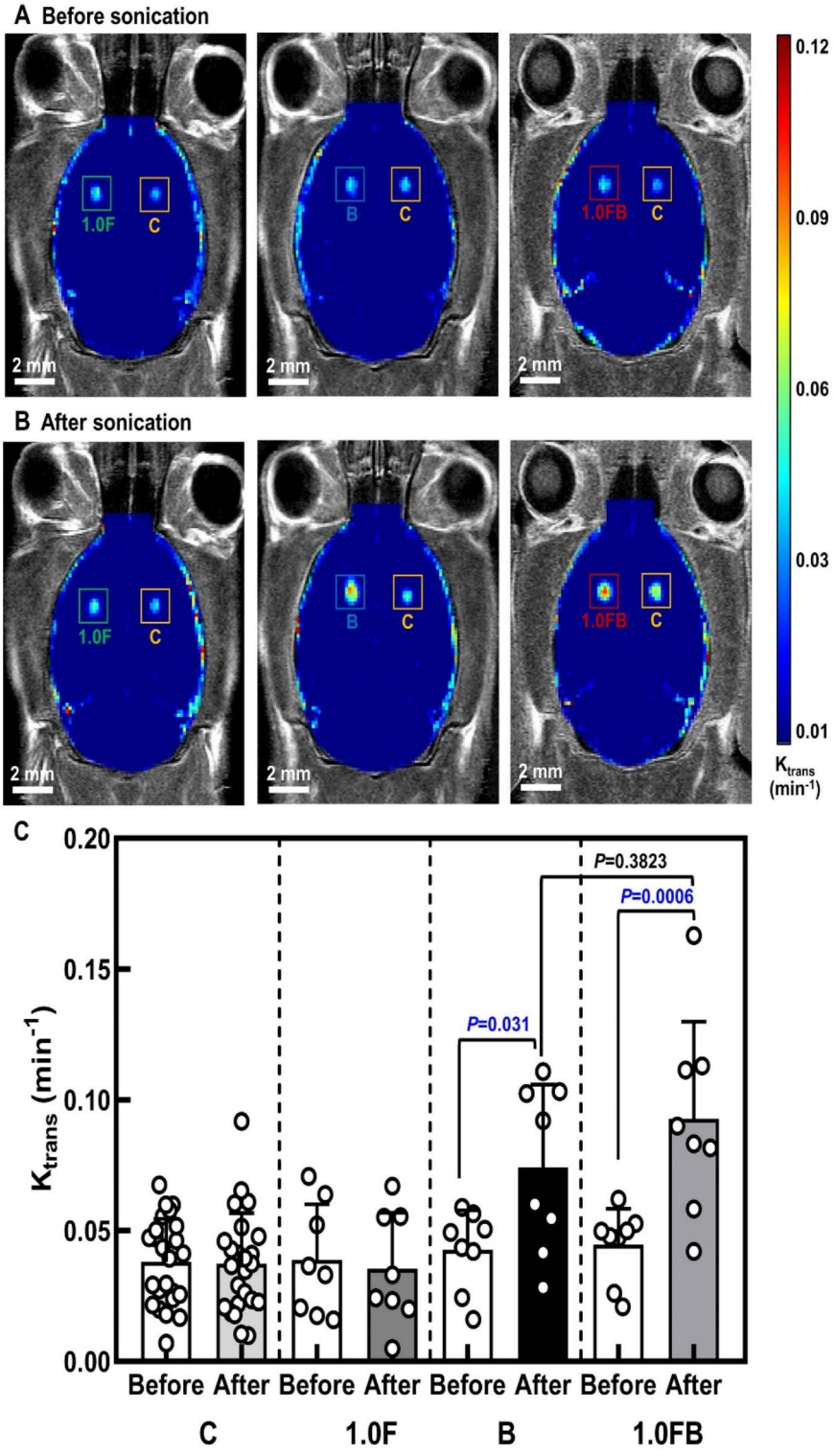

Fig. 4. Representative K_{trans} map of "1.0F" (green box), "B" (blue box), and "1.0FB" (red box) protocol and the contralateral region (yellow box) (**A**) before and (**B**) after sonication. The color bar indicates the BBB permeability. (**C**) The group averaged mean K_{trans} value before and after the sonication. Scale bars represent 2 mm. (K_{trans} value: "C" $n = 4$; "1.0F" $n = 4$; "B" $n = 4$; "1.0FB" $n = 4$).

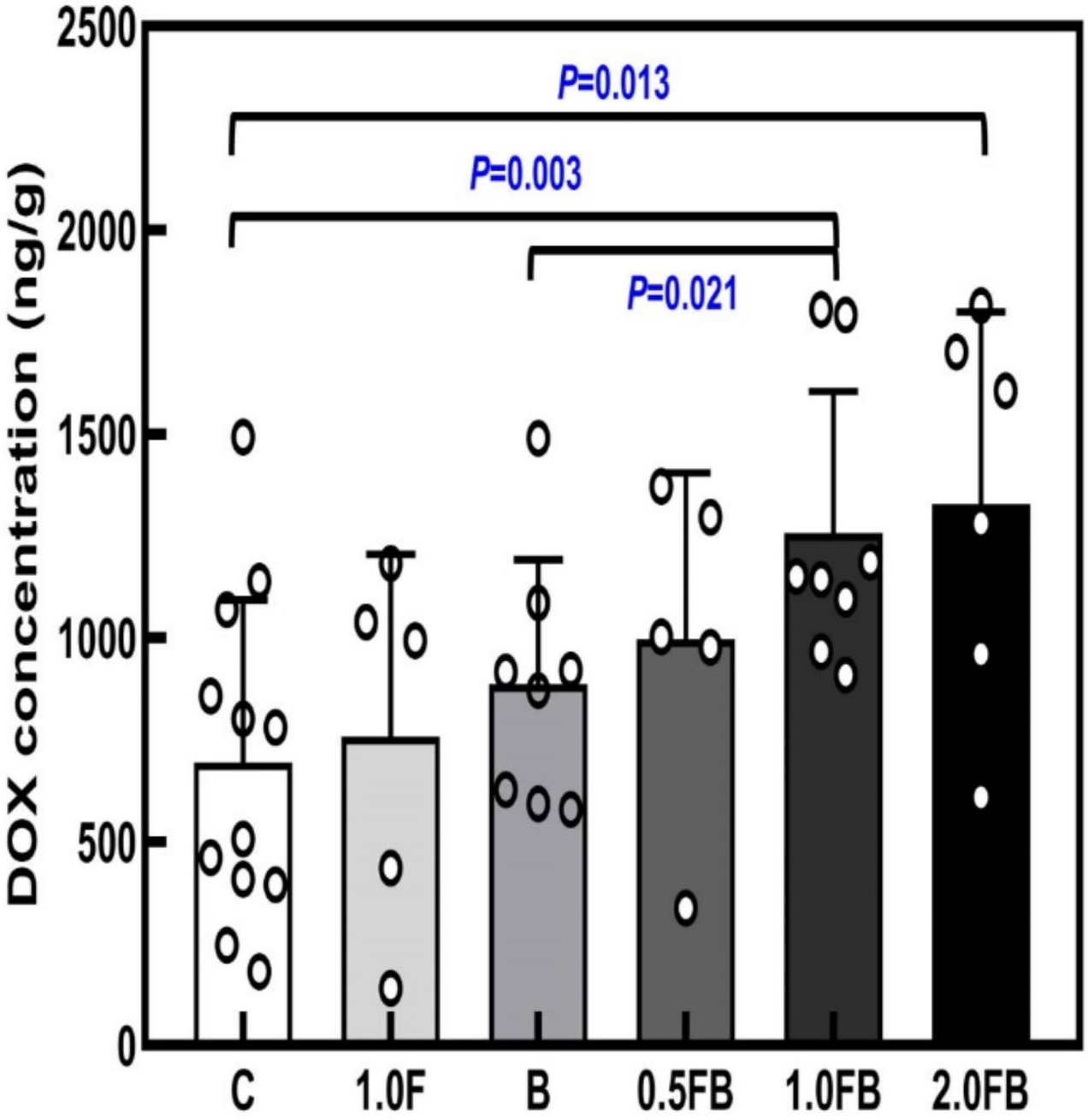

Fig. 5. Comparison of the DOX quantification measured 24 h after sonication using a fluorometric detector. The bars represent the average DOX concentration for each group ("C", $n = 12$; "1.0F", $n = 5$; "B", $n = 8$; "0.5FB", $n = 5$; "1.0FB", $n = 8$, "2.0FB", $n = 6$), while the dots represent individual cases. Data are expressed as means ± SD. Two-way ANOVA and Tukey's tests for the multiple comparisons were used. Statistical significance was determined using the Mann-Whitney U test.

Compared to the conventional BBBD protocol "B", the addition of ultrasound stimulation resulted in a 2.08-fold increase in BTB permeability. This is consistent with previous findings, where additional sonication prior to BBBD increased the average K_{trans} in normal tissue by 1.36-fold compared to the conventional BBBD protocol[27]. Despite differences in the permeability characteristics of the BBB/BTB between the current tumor model and normal brain tissue, the addition of an extra sonication step prior to BBBD consistently produced a comparable increase in permeability.

The amount of chemotherapeutic agent delivered was also compared after sonication using each protocol (Fig. 5). In order to minimize experimental bias, animals with a tumor size of less than 20% difference were selected and used (and tumor diameter between 1.5 ~ 2.0 mm). The delivery of DOX to the target tumor region sonicated using the "1.0FB" protocol was 1.81-fold higher than that achieved with the conventional BBBD protocol

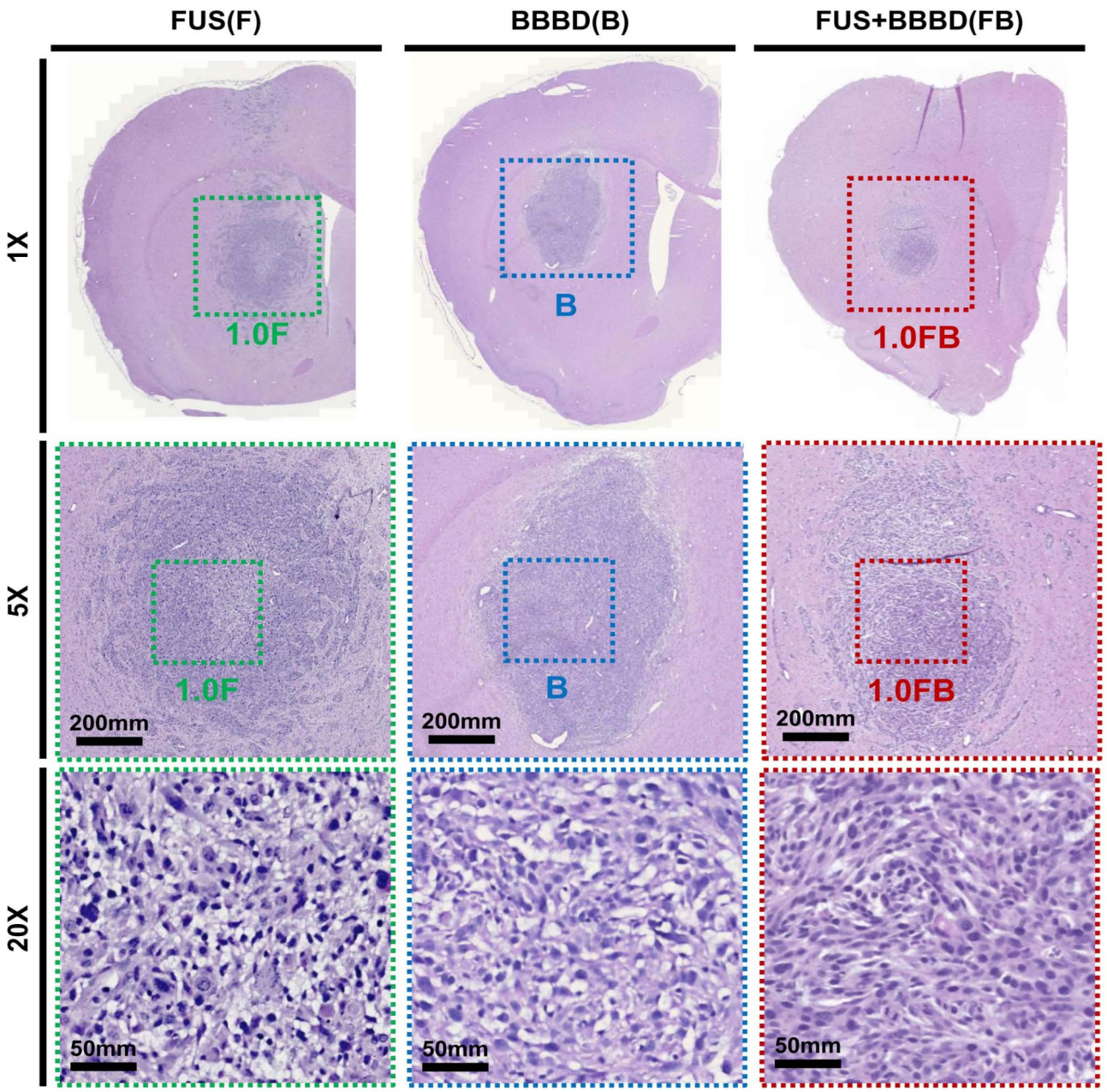

Fig. 6. Histopathological analysis of the rat brain tumor after the "1.0F", "B", and "1.0FB" with H&E staining. The images indicate representative photomicrographs of "1.0F", "B", and "1.0FB". The 5× and 20× magnified images were obtained from a whole-brain section specimen. Scale bars represent 50 μm at 5× magnified images and 100 μm at 20× magnified images, respectively. ("1.0F", Green box; "B", Blue box; "1.0FB", Red box)

"B". While the 'FUS + BBBD protocol' demonstrated trends toward higher permeability (K_{trans}) compared to the 'BBBD protocol', the differences were not statistically significant. However, DOX delivery showed a statistically significant improvement ($p = 0.0021$), providing strong evidence for the efficacy of the 'FUS + BBBD protocol' in enhancing drug delivery to tumor regions. These results suggest that the additional focused ultrasound stimulation may contribute to improved therapeutic outcomes, despite the inherent variability in tumor-associated vasculature.

Future studies with larger sample sizes and advanced methodologies, such as refined imaging techniques and histological validation, will be necessary to further investigate these findings and quantify the full potential of the 'FUS + BBBD protocol' in overcoming challenges associated with tumor heterogeneity[41–43].

An additional sonication step prior to BBBD was shown to enhance BBB/BTB permeability, thereby increasing the overall delivery of chemotherapeutic agents in the tumor model. To assess the safety of this new protocol in the brain tumor environment, histopathological examination of brain tissue was performed using

standard H&E staining to evaluate potential brain damage[44,45]. As shown in Fig. 6 no significant differences were observed in the "1.0FB" group compared to the "B" and "1.0F" groups.

The enhancement of brain permeability by adding an extra sonication step prior to conventional BBBD (ultrasound with intravenously injected microbubbles) may increase sensitivity to acoustic energy by affecting the cytoskeleton and extracellular matrix through dynamic remodeling and matrix degradation[46]. Another possibility is that the increased permeability results from the expansion of extracellular and perivascular spaces, rather than changes in the BBB itself. Recent studies have highlighted the role of mechanical stress on mechanosensitive calcium ion channels[47–50]. Among these, TRP channels are widely expressed and activated by various stimuli, with the mammalian TRP channel family divided into six subfamilies: canonical (TRPC1-7), vanilloid (TRPV1-6), melastatin (TRPM1-8), polycystin (TRPP1-5), mucolipin (TRPML1-3), and ankyrin (TRPA1)[51–53]. These ion channels are known to compromise BBB integrity, suggesting that prior FUS stimulation may enhance BBB disruption, potentially explaining the current findings[49]. Further studies are required to fully understand the underlying mechanism of the drug delivery enhancement. Furthermore, these mechanotransductive effects are likely to be time-dependent, potentially altering the microenvironment and influencing the subsequent efficacy of the BBBD protocol. To address this limitation, future studies should systematically evaluate the temporal dynamics following sonication to identify the optimal time interval for BBBD application. Such investigations would provide critical insights into enhancing therapeutic delivery while minimizing off-target effects.

DOX is widely used in chemotherapeutic drug delivery studies. However, other therapeutic agents that may benefit from enhanced drug delivery were not evaluated in this study. For instance, TMZ is the primary treatment option for gliomas. It is a relatively small lipophilic molecule that can cross the BBB[54]. It has been shown that TMZ levels in the brain and cerebrospinal fluid reach up to 20% of the drug plasma concentration[55]. However, the therapeutic potential of TMZ for glioma treatment is limited by its short half-life (1.8 h). This requires continuous drug administration to maintain the therapeutic concentration of the drug in tumor tissue and to optimize therapeutic potential[56]. The proposed FUS + BBBD protocol may offer a safe and effective method to deliver TMZ in the near future. In this study, blood sampling to measure systemic concentrations of doxorubicin (DOX) at key time points, such as the time of sonication and sacrifice, was not performed. Blood sampling could have provided additional data to normalize DOX delivery as a percentage of the injected dose, facilitating more accurate intergroup comparisons. While this aspect was not included in the current study, future investigations will incorporate pharmacokinetic analyses, including blood sampling at key intervals, to provide a more comprehensive understanding of DOX distribution and clearance. Addressing this limitation will enhance the robustness of intergroup comparisons and improve our interpretation of therapeutic outcomes. In addition, only a well-characterized 9 L gliosarcoma that is both highly immunogenic and poorly infiltrative was used in this study[28,57,58]. Future studies should include a broader range of brain tumor models, such as glioma, glioblastoma, medulloblastoma, and brain metastasis, as each tumor type may present different characteristics due to tumor heterogeneity[24]. Finally, further studies are required to validate the effect of mechanosensitive forces on calcium ion channels[49,50].

Concluding remarks

In conclusion, while the addition of mechanical stress from ultrasound stimulation prior to conventional BBBD did not result in a statistically significant increase in permeability, a trend toward enhanced permeability was observed. Moreover, the significant improvement in doxorubicin delivery suggests that the proposed "FUS + BBBD protocol" may facilitate drug delivery to brain tumors. These findings align with previous studies indicating that focused ultrasound can enhance the delivery of therapeutic agents across the blood-brain and blood-tumor barriers. Further research is necessary to validate these findings and to elucidate the underlying biomolecular and cellular mechanisms, both in preclinical studies and potential clinical applications.

Data availability

All data generated or analyzed during this study are included in this published article. The datasets used and/or analyzed during the current study are also available from the corresponding author upon reasonable request.

Received: 4 October 2024; Accepted: 28 January 2025
Published online: 24 February 2025

References

1. Deeken, J. F. & Loscher, W. The blood-brain barrier and cancer: transporters, treatment, and Trojan horses. *Clin. Cancer Res.* **13**, 1663–1674. https://doi.org/10.1158/1078-0432.ccr-06-2854 (2007).
2. Achrol, A. S. et al. Brain metastases. *Nat. Revi. Dis. Primers*. **5** https://doi.org/10.1038/s41572-018-0055-y (2019).
3. Quail, D. F. & Joyce, J. A. The Microenvironmental Landscape of Brain tumors. *Cancer Cell.* **31**, 326–341. https://doi.org/10.1016/j.ccell.2017.02.009 (2017).
4. Hobbs, S. K. et al. Regulation of transport pathways in tumor vessels: role of tumor type and microenvironment. *Proc. Natl. Acad. Sci. U.S.A.* **95**, 4607–4612. https://doi.org/10.1073/pnas.95.8.4607 (1998).
5. Monsky, W. L. et al. Role of host microenvironment in angiogenesis and microvascular functions in human breast cancer xenografts: mammary fat pad versus cranial tumors. *Clin. Cancer Res.* **8**, 1008–1013 (2002).
6. Pitz, M. W., Desai, A., Grossman, S. A. & Blakeley, J. O. Tissue concentration of systemically administered antineoplastic agents in human brain tumors. *J. Neuro-oncol.* **104**, 629–638. https://doi.org/10.1007/s11060-011-0564-y (2011).
7. Sarkaria, J. N. et al. Is the blood-brain barrier really disrupted in all glioblastomas? A critical assessment of existing clinical data. *Neuro-oncology* **20**, 184–191. https://doi.org/10.1093/neuonc/nox175 (2018).
8. Agarwal, S., Sane, R., Oberoi, R., Ohlfest, J. R. & Elmquist, W. F. Delivery of molecularly targeted therapy to malignant glioma, a disease of the whole brain. *Expert Rev. Mol. Med.* **13**, e17. https://doi.org/10.1017/s1462399411001888 (2011).
9. Gabathuler, R. Approaches to transport therapeutic drugs across the blood-brain barrier to treat brain diseases. *Neurobiol. Dis.* **37**, 48–57. https://doi.org/10.1016/j.nbd.2009.07.028 (2010).

10. Bunevicius, A., McDannold, N. J. & Golby, A. J. Focused Ultrasound Strategies for Brain Tumor Therapy. *Operative neurosurgery. (Hagerstown Md)*. **19**, 9–18. https://doi.org/10.1093/ons/opz374 (2020).
11. Song, R. et al. Selection of rAAV vectors that cross the human blood-brain barrier and target the central nervous system using a transwell model. *Mol. Therapy Methods Clin. Dev.* **27**, 73–88. https://doi.org/10.1016/j.omtm.2022.09.002 (2022).
12. Zhang, W., Mehta, A., Tong, Z., Esser, L. & Voelcker, H. Development of polymeric nanoparticles for blood-brain barrier transfer-strategies and challenges. *Adv. Sci. (Weinheim Baden-Wurttemberg Germany)*. **8**, 2003937. https://doi.org/10.1002/advs.202003937 (2021).
13. Wang, Y. et al. Engineered exosomes with enhanced stability and delivery efficiency for glioblastoma therapy. *J. Controlled Release*. **368**, 170–183. https://doi.org/10.1016/j.jconrel.2024.02.015 (2024).
14. Dong, X. Current strategies for Brain Drug Delivery. *Theranostics* **8**, 1481–1493. https://doi.org/10.7150/thno.21254 (2018).
15. Hollon, T. Researchers and regulators reflect on first gene therapy death. *Am. J. Ophthalmol.* **129**, 701. https://doi.org/10.1016/s0002-9394(00)00442-6 (2000).
16. Check, E. Gene therapy put on hold as third child develops cancer. *Nature* **433**, 561. https://doi.org/10.1038/433561a (2005).
17. Wilhelm, S. et al. Analysis of nanoparticle delivery to tumours. *Nat. Reviews Mater.* **1** https://doi.org/10.1038/natrevmats.2016.14 (2016).
18. Kinoshita, M., McDannold, N., Jolesz, F. A. & Hynynen, K. Noninvasive localized delivery of Herceptin to the mouse brain by MRI-guided focused ultrasound-induced blood-brain barrier disruption. *Proc. Natl. Acad. Sci. U.S.A.* **103**, 11719–11723. https://doi.org/10.1073/pnas.0604318103 (2006).
19. Park, J., Aryal, M., Vykhodtseva, N., Zhang, Y. Z. & McDannold, N. Evaluation of permeability, doxorubicin delivery, and drug retention in a rat brain tumor model after ultrasound-induced blood-tumor barrier disruption. *J. Controlled Rel.*. **250**, 77–85 (2017).
20. Wei, K. C. et al. Focused ultrasound-induced blood-brain barrier opening to enhance temozolomide delivery for glioblastoma treatment: a preclinical study. *PloS One*. **8**, e58995. https://doi.org/10.1371/journal.pone.0058995 (2013).
21. Mei, J. et al. Experimental study on targeted methotrexate delivery to the rabbit brain via magnetic resonance imaging-guided focused ultrasound. *J. Ultrasound Med.* **28**, 871–880. https://doi.org/10.7863/jum.2009.28.7.871 (2009).
22. Dréan, A. et al. Temporary blood-brain barrier disruption by low intensity pulsed ultrasound increases carboplatin delivery and efficacy in preclinical models of glioblastoma. *J. Neurooncol.* **144**, 33–41. https://doi.org/10.1007/s11060-019-03204-0 (2019).
23. Arsiwala, T. A. et al. Ultrasound-mediated disruption of the blood tumor barrier for improved therapeutic delivery. *Neoplasia (New York N Y)*. **23**, 676–691. https://doi.org/10.1016/j.neo.2021.04.005 (2021).
24. Arvanitis, C. D., Ferraro, G. B. & Jain, R. K. The blood-brain barrier and blood-tumour barrier in brain tumours and metastases. *Nat. Rev. Cancer*. **20**, 26–41. https://doi.org/10.1038/s41568-019-0205-x (2020).
25. McMahon, D. & Hynynen, K. Acute Inflammatory Response following increased blood-brain Barrier Permeability Induced by Focused Ultrasound is dependent on Microbubble Dose. *Theranostics* **7**, 3989–4000. https://doi.org/10.7150/thno.21630 (2017).
26. Kovacs, Z. I. et al. Disrupting the blood-brain barrier by focused ultrasound induces sterile inflammation. *Proc. Natl. Acad. Sci. U.S.A.* **114**, E75–e84. https://doi.org/10.1073/pnas.1614777114 (2017).
27. Jung, B., Huh, H., Lee, E. H., Han, M. & Park, J. An advanced focused ultrasound protocol improves the blood-brain barrier permeability and doxorubicin delivery into the rat brain. *J. Controlled Release*. **315**, 55–64. https://doi.org/10.1016/j.jconrel.2019.10.044 (2019).
28. Barth, R. F. & Kaur, B. Rat brain tumor models in experimental neuro-oncology: the C6, 9L, T9, RG2, F98, BT4C, RT-2 and CNS-1 gliomas. *J. Neurooncol.* **94**, 299–312. https://doi.org/10.1007/s11060-009-9875-7 (2009).
29. Tamargo, R. J. et al. Interstitial chemotherapy of the 9L gliosarcoma: controlled release polymers for drug delivery in the brain. *Cancer Res.* **53**, 329–333 (1993).
30. Cho, H. et al. Localized down-regulation of P-glycoprotein by focused ultrasound and microbubbles induced blood-brain barrier disruption in rat brain. *Sci. Rep.* **6**, 31201 (2016).
31. Treat, L. H. et al. Targeted delivery of doxorubicin to the rat brain at therapeutic levels using MRI-guided focused ultrasound. *Int. J. Cancer*. **121**, 901–907. https://doi.org/10.1002/ijc.22732 (2007).
32. Park, J., Zhang, Y., Vykhodtseva, N., Jolesz, F. A. & McDannold, N. J. The kinetics of blood brain barrier permeability and targeted doxorubicin delivery into brain induced by focused ultrasound. *J. Controlled Release*. **162**, 134–142. https://doi.org/10.1016/j.jconrel.2012.06.012 (2012).
33. Barboriak, D. P., Padua, J. R. M. A. O., York, G. E. & Viglianti, B. L. M.W. Dewhirst. Standardized software for calculation of Ktrans and vp from dynamic T1-weighted MR images. (2004).
34. Bachur, N. R., Moore, A. L., Bernstein, J. G. & Liu, A. Tissue distribution and disposition of daunomycin (NCS-82151) in mice: fluorometric and isotopic methods. *Cancer Chemother. Rep.* **54**, 89–94 (1970).
35. Mainprize, T. et al. Blood-brain barrier opening in primary brain tumors with non-invasive MR-Guided focused Ultrasound: a clinical safety and feasibility study. *Sci. Rep.* **9**, 321. https://doi.org/10.1038/s41598-018-36340-0 (2019).
36. Idbaih, A. et al. Safety and feasibility of repeated and transient blood-brain barrier disruption by Pulsed Ultrasound in patients with recurrent glioblastoma. *Clin. Cancer Res.* **25**, 3793–3801. https://doi.org/10.1158/1078-0432.Ccr-18-3643 (2019).
37. Carpentier, A. et al. Clinical trial of blood-brain barrier disruption by pulsed ultrasound. *Sci. Transl. Med.* **8**, 343re342–343re342 (2016).
38. Aryal, M., Arvanitis, C. D., Alexander, P. M. & McDannold, N. Ultrasound-mediated blood-brain barrier disruption for targeted drug delivery in the central nervous system. *Adv. Drug Deliv. Rev.* **72**, 94–109. https://doi.org/10.1016/j.addr.2014.01.008 (2014).
39. Hynynen, K., McDannold, N., Vykhodtseva, N. & Jolesz, F. A. Noninvasive MR imaging-guided focal opening of the blood-brain barrier in rabbits. *Radiology* **220**, 640–646. https://doi.org/10.1148/radiol.2202001804 (2001).
40. Meairs, S. Facilitation of drug transport across the blood-brain barrier with Ultrasound and Microbubbles. *Pharmaceutics* **7**, 275–293. https://doi.org/10.3390/pharmaceutics7030275 (2015).
41. Ahishali, B. & Kaya, M. Evaluation of blood-brain Barrier Integrity using vascular permeability markers: Evans Blue, Sodium Fluorescein, Albumin-Alexa Fluor conjugates, and Horseradish Peroxidase. *Methods in molecular biology. N J)*. **2367**, 87–103. https://doi.org/10.1007/7651_2020_316 (2021). Clifton.
42. Salehi, A. et al. Therapeutic enhancement of blood-brain and blood-tumor barriers permeability by laser interstitial thermal therapy. *Neuro-oncology Adv.* **2**, vdaa071. https://doi.org/10.1093/noajnl/vdaa071 (2020).
43. Arrieta, V. A. et al. Ultrasound-mediated delivery of doxorubicin to the brain results in immune modulation and improved responses to PD-1 blockade in gliomas. *Nat. Commun.* **15**, 4698. https://doi.org/10.1038/s41467-024-48326-w (2024).
44. Li, Y. et al. Hematoxylin and eosin staining of intact tissues via delipidation and ultrasound. *Sci. Rep.* **8**, 12259. https://doi.org/10.1038/s41598-018-30755-5 (2018).
45. Chan, J. K. The wonderful colors of the hematoxylin-eosin stain in diagnostic surgical pathology. *Int. J. Surg. Pathol.* **22**, 12–32. https://doi.org/10.1177/1066896913517939 (2014).
46. Muiznieks, L. D. & Keeley, F. W. Molecular assembly and mechanical properties of the extracellular matrix: a fibrous protein perspective. *Biochim. Biophys. Acta (BBA) Mol. Basis Dis.* **1832**, 866–875 (2013).
47. Kubanek, J. et al. Ultrasound modulates ion channel currents. *Sci. Rep.* **6**, 24170. https://doi.org/10.1038/srep24170 (2016).
48. Qiu, Z. et al. The Mechanosensitive Ion Channel Piezo1 significantly mediates in Vitro Ultrasonic stimulation of neurons. *iScience* **21**, 448–457. https://doi.org/10.1016/j.isci.2019.10.037 (2019).

49. Yoo, S., Mittelstein, D. R., Hurt, R., Lacroix, J. & Shapiro, M. G. Focused ultrasound excites neurons via mechanosensitive calcium accumulation and ion channel amplification. *bioRxiv*, 2020.2005.2019.101196. https://doi.org/10.1101/2020.05.19.101196 (2020).
50. Berrout, J., Jin, M. & O'Neil, R. G. Critical role of TRPP2 and TRPC1 channels in stretch-induced injury of blood-brain barrier endothelial cells. *Brain Res.* **1436**, 1–12. https://doi.org/10.1016/j.brainres.2011.11.044 (2012).
51. Samanta, A., Hughes, T. E. T. & Moiseenkova-Bell, V. Y. Transient receptor potential (TRP) channels. *Subcell. Biochem.* **87**, 141–165. https://doi.org/10.1007/978-981-10-7757-9_6 (2018).
52. Li, H. T. R. P., Channel & Classification *Adv. Exp. Med. Biol.* **976**, 1–8, doi:https://doi.org/10.1007/978-94-024-1088-4_1 (2017).
53. Christensen, A. P. & Corey, D. P. TRP channels in mechanosensation: direct or indirect activation? *Nat. Rev. Neurosci.* **8**, 510–521. https://doi.org/10.1038/nrn2149 (2007).
54. Agarwala, S. S. & Kirkwood, J. M. Temozolomide, a novel alkylating agent with activity in the central nervous system, may improve the treatment of advanced metastatic melanoma. *Oncologist* **5**, 144–151. https://doi.org/10.1634/theOncologist.5-2-144 (2000).
55. Ostermann, S. et al. Plasma and cerebrospinal fluid population pharmacokinetics of temozolomide in malignant glioma patients. *Clin. Cancer Res.* **10**, 3728–3736. https://doi.org/10.1158/1078-0432.Ccr-03-0807 (2004).
56. Berrocal, A. et al. Extended-schedule dose-dense temozolomide in refractory gliomas. *J. Neurooncol.* **96**, 417–422. https://doi.org/10.1007/s11060-009-9980-7 (2010).
57. Doblas, S. et al. Glioma morphology and tumor-induced vascular alterations revealed in seven rodent glioma models by in vivo magnetic resonance imaging and angiography. *J. Magn. Reson. Imaging: JMRI.* **32**, 267–275. https://doi.org/10.1002/jmri.22263 (2010).
58. Doblas, S. et al. In vivo characterization of several rodent glioma models by 1H MRS. *NMR Biomed.* **25**, 685–694. https://doi.org/10.1002/nbm.1785 (2012).

Acknowledgements
We would like to appreciate Yuri Hong who supported biological assay in this study.

Author contributions
H.J. Choi: Methodology, Histopathological sample preparation, Analysis and validation, Writing-draft preparation, Writing-review and editingM. Han: Methodology, In vivo preclinical experiment, Analysis and validation, Writing-draft preparation, Writing-review and editingB. Jung: Methodology, In vivo preclinical experiment, Writing-draft preparationH. Huh: Analysis and validation, Writing-draft preparationE.-h. Lee: Analysis and validation, Writing-review and editingJ.-r. Choi: Analysis and validation, Writing-review and editingJ. Park: Supervision, Conceptualization, Funding acquisition, Methodology, Analysis and validation, Writing-draft preparation, Writing-review and editing.

Declarations

Competing interests
The authors declare no competing interests.

Additional information
Correspondence and requests for materials should be addressed to J.P.

Reprints and permissions information is available at www.nature.com/reprints.

Publisher's note Springer Nature remains neutral with regard to jurisdictional claims in published maps and institutional affiliations.